TITLE

Reactive Oxygen Detoxification Contributes to *Mycobacterium abscessus* Antibiotic Survival

AUTHORS

Nicholas A. Bates[1,2], Ronald Rodriguez[3,4], Rama Drwich[1], Abigail Ray[5], Sarah A. Stanley[3], Bennett H. Penn[1,6]*

AFFILIATIONS:

1. Department of Internal Medicine, University of California, Davis, California, USA
2. Graduate Group in Immunology, University of California, Davis, California, USA
3. Department of Molecular & Cell Biology, University of California, Berkeley, California, USA
4. Department of Plant & Microbial Biology, University of California, Berkeley, California, USA
5. Microbiology Graduate Group, University of California, Davis, California, USA
6. Department of Medical Microbiology and Immunology, University of California, Davis, California, USA

*Corresponding author

Email: bhpenn@ucdavis.edu

ABSTRACT

When a population of bacteria encounter a bactericidal antibiotic most cells die rapidly. However, a sub-population, known as “persister cells”, can survive for prolonged periods in a non-growing, but viable, state. Persister cell frequency is dramatically increased by stresses such as nutrient deprivation, but it is unclear what pathways are required to maintain viability, and how this process is regulated. To identify the genetic determinants of antibiotic persistence in mycobacteria, we

carried out transposon mutagenesis high-throughput sequencing (Tn-Seq) screens in *Mycobacterium abscessus* (*Mabs*). This analysis identified genes essential in both spontaneous and stress-induced persister cells, allowing the first genetic comparison of these states in mycobacteria, and unexpectedly identified multiple genes involved in the detoxification of reactive oxygen species (ROS). We found that endogenous ROS were generated following antibiotic exposure, and that the KatG catalase-peroxidase contributed to survival in both spontaneous and starvation-induced persisters. We also found that that hypoxia significantly impaired bacterial killing, and notably, in the absence of oxygen, KatG became dispensable. Thus, the lethality of some antibiotics is amplified by toxic ROS accumulation, and persister cells depend on detoxification systems to remain viable.

INTRODUCTION

A key goal of antibiotic therapy is the complete eradication of the pathogen. While many common infections respond rapidly to antibiotics, and high cure rates are achieved with 1-2 weeks of therapy[1,2], there are also infections where bacterial clearance is either very slow, or frequently incomplete. This challenge is exemplified by mycobacterial infections, where treatment courses extend from months to years to prevent relapse.

While the ability of mycobacteria to escape antibiotic-mediated killing is multifactorial, the phenomenon of antibiotic “persistence” is likely an important contributor[3-6]. Studies on penicillin dating from the 1940s noted that when a population of susceptible bacteria were exposed to a bactericidal antibiotic, the majority of the population died within a few hours, but that a small sub-population of ‘persisters’ remained viable for over a week[7]. Importantly, these persister cells had not acquired a mutation conferring heritable antibiotic resistance, and do not grow in the presence of the antibiotic. Rather, they have entered into a readily-reversable epigenetic state[8-10] where, despite antibiotic-mediated inhibition of critical processes, they are able to survive. Virtually all

53 bacterial species display the ability to form persister cells, and their development is strongly
54 induced in response to stresses such as nutrient deprivation or acidic pH[6-7,11-12]. Notably, these
55 same stresses are encountered in the lysosome of an activated immune cell[13], and studies of
56 pathogens isolated from activated macrophages indeed show a strong immune-mediated
57 increase in persister cells[5,14]. Thus, paradoxically, the immune system may actually impede
58 bacterial eradication by antibiotics.
59
60 Persister formation has been studied extensively in model systems such as *Escherichia coli*,
61 which has provided important insights, but also highlighted uncertainties of current models.
62 Several different pathways have been implicated in *E. coli* persister formation, including the HipBA
63 toxin-antitoxin system[15], guanosine pentaphosphate ((p)ppGpp) synthesis by RelA/SpoT
64 enzymes[16,17], and Lon protease[16]. In each of these models, the postulated mechanism is to halt
65 cell division and render the process targeted by antibiotics non-essential. However, important
66 questions remain unanswered. It is unclear how persister cells remain viable when critical
67 processes such as transcription or translation are arrested by antibiotics, as well as how the
68 process is regulated and induced by stress.
69
70 Even the mechanism of cell death following antibiotic exposure itself remains uncertain, and
71 somewhat controversial. Historically, antibiotics have been presumed to kill bacteria as a direct
72 result of inhibition of their target molecule, such as β-lactam antibiotics disrupting cell wall integrity,
73 directly leading to mechanical cell lysis[18]. However, a number of studies, largely from *E. coli*, have
74 suggested that reactive oxygen species (ROS) accumulation triggered by antibiotic stress might
75 also contribute to cell death[10,19-20]. Conversely, other studies have found no such association[21,22],
76 leaving the role of ROS in antibiotic-mediated cell death unresolved.
77

78 Studying persister cell physiology in mycobacterial pathogens offers several advantages.
79 Mycobacterial persister cells are particularly resilient, as *Mycobacterium smegmatis* (*Msmeg*) and
80 *Mycobacterium tuberculosis (Mtb)* persisters can endure many weeks of antibiotic exposure[10,23-
81 24]. Clinically, mycobacterial infections are difficult to eradicate. Fully-susceptible *Mtb* requires
82 multiple antibiotics for four months or longer[25-26], whereas non-tuberculous mycobacteria typically
83 require treatment for 12-18 months and have a relapse rates of roughly 50%[27]. *Mycobacterium*
84 *abscessus* (*Mabs*) is among the most difficult of all bacterial pathogens to treat, because in
85 addition to the possibility of forming persister cells, it is intrinsically resistant to many classes of
86 antibiotics, leaving few treatment options[28]. This leads to the use of antibiotics with greater toxicity
87 to patients, and a need to use these agents for prolonged periods to prevent relapse. Thus,
88 identifying the genes that *Mabs* persister cells rely on for survival could be beneficial by
89 highlighting pathways that might be targeted therapeutically to eliminate persister cells.
90
91 Previous genetic screens have studied antibiotic responses in mycobacteria, with some
92 evaluating heritable resistance, and others investigating persister cell formation. Several studies
93 of genetic resistance have successfully used either transposon mutagenesis with high-throughput
94 sequencing of insertion sites (Tn-Seq) or CRISPR-based transcriptional repression with high-
95 throughput sequencing of guide RNAs (CRISPRi) to identify genes promoting growth in sub-
96 inhibitory concentrations of antibiotic. These studies have provided insights such as the
97 importance of cell membrane permeability controlling antibiotic penetration into the cytoplasm[29-
98 31]. Persister cell formation has proven challenging to study, likely because their low frequency leads
99 to population bottlenecks that confound genetic analysis. Although screens in *Mtb* have been
100 conducted in macrophages and mice, and genes such as *glpK* and *cinA* identified, overall the
101 number of mutants isolated in these screens has been low[32-34]. There has been one highly-
102 effective in vitro Tn-Seq study of rifampin survival in *Mtb* that isolated over 100 mutants[19],
103 demonstrating the feasibility of genetic screening in this context. However, whether these

104 phenotypes seen with rifampin in *Mtb* extend to other organisms and other antibiotics remains to
105 be determined.
106
107 Here, we study persister cell formation in *Mabs*, and describe the results of genome-wide Tn-seq
108 screens seeking to identify the genes required for both spontaneous and starvation-induced
109 antibiotic persistence. We identified diverse pathways contributing to persister cell survival, and
110 unexpectedly, observed a prominent role for ROS detoxifying factors such as the catalase-
111 peroxidase enzyme KatG, which contributed to both spontaneous and starvation-induced
112 persistence. We found that endogenous ROS were generated following antibiotic exposure, and
113 that hypoxia significantly impaired bacterial killing. Thus, the lethality of some antibiotics is
114 amplified by toxic ROS accumulation, and persister cells require detoxification systems.
115
116 **RESULTS**
117 **Starvation-induced persister cell formation in mycobacteria**
118 We first sought to develop conditions suitable for genetic analysis of antibiotic persistence in
119 mycobacteria. Genetic screens examining persister cell physiology faces two inherent obstacles.
120 First, persister cells are rare in unstressed bacterial populations, and antibiotic-mediated cell
121 death creates population bottlenecks that obscure mutant phenotypes. Second, most
122 mycobacterial populations contain spontaneous drug-resistant mutants that can expand if the
123 population is exposed to a single antibiotic. To overcome these obstacles, we sought to establish
124 large-scale, high-density culture conditions to prevent genetic bottlenecks, and used multiple
125 antibiotics to suppress expansion of spontaneous drug-resistant mutants. We began by assessing
126 the feasibility of this approach using wild-type *Msmeg.* We exposed the cells to either the
127 combination of rifampin, isoniazid, and ethambutol (RIF/INH/EMB) used to treat *Mtb*, or to the
128 combination of tigecycline and linezolid (TIG/LZD), two translation-inhibiting antibiotics frequently
129 used to treat *Mabs*[27,35], and empirically determined the minimum-inhibitory concentrations (MICs)

130 each antibiotic under the high-density culture conditions that would be needed for genetic analysis
131 of antibiotic persister cells. Both antibiotic combinations reduced the bacterial population >1000-
132 fold within 72h (Figure 1A). We then evaluated both spontaneous and stress-induced persister
133 cell formation under these conditions in *Msmeg*. We compared logarithmically growing (mid-log)
134 cultures in 7H9 rich media to cultures starved for 2 days in PBS prior to addition of antibiotics.
135 Consistent with expectations, we found a marked increase in the frequency of persister cells in
136 starved cultures, with a 100-fold increase in survival following TIG/LZD exposure and a 10,000-
137 fold increase following RIF/INH/EMB exposure (Figure 1A).
138
139 We next examined two species of pathogenic mycobacteria to similarly assess stress-induced
140 persister formation under these conditions, as has been reported previously[36-39]. We again
141 compared cells starved in PBS to mid-log cells growing 7H9, and found that cultures of wild-type
142 *Mabs* (ATCC 19977 strain) and *Mtb* (Erdman) also displayed dramatic increases in the frequency
143 of persister cells in nutrient-deprived cultures (Figure 1B,C). Notably, for *Mabs* and *Msmeg,* the
144 development of these persister cells required an adaptation period of several days under
145 starvation conditions, as formation of persister cells was dramatically impaired if cells were shifted
146 immediately into nutrient-deficient conditions with antibiotics, suggesting that a regulated process
147 needed to be completed (Figure 1D-F).
148
149 **Identification of pathways needed for persister formation in *Mabs***
150 We used these conditions to carry out Tn-Seq screens in *Mabs* to identify genes necessary for
151 forming both spontaneous and starvation-induced persister cells. We conducted the screen using
152 a *Mabs Himar1* Tn library comprised of ~55,000 mutations across all 4,992 non-essential *Mabs*
153 genes in strain ATCC 19977[29]. We maintained cells in log-phase growth in 7H9 rich media, or
154 starved cells in PBS as described above, and then exposed them to TIG/LZD for 6 days (Figure
155 2A), a point at which spontaneous persister cells comprise the majority of the population (Figure

156 1C). Following antibiotic exposure cells were then washed and placed in antibiotic-free liquid
157 media to recover, genomic DNA was isolated, and Tn insertion sites sequenced. We then used
158 TRANSIT software[40] to quantify the abundance of each Tn mutant across different conditions and
159 identify mutants with statistically-significant differences in distribution, in order to identify essential
160 genes in both spontaneous and stress-induced antibiotic persister cells. We identified 277 *Mabs*
161 genes required for surviving TIG/LZD exposure in rich media, 271 genes required for survival
162 during starvation and 362 genes required to survive the combined exposure to antibiotics and
163 starvation using criteria for significance of Log_2 fold-change > 0.5 and Benjamini–Hochberg
164 adjusted p-value (p-adj.) ≤ 0.05 (Figure 2B-E). Of the genes required for antibiotic persistence,
165 ~60% were required in both nutrient-replete and starvation states, although condition-specific
166 determinants were also seen (Figure 2F). As expected, we identified genes with already-
167 established functions in antibiotic responses, including MAB_2752 and MAB_2753 which are both
168 homologs of known antibiotic transporters in *Mtb,* and tetracycline-responsive transcription factors
169 such as MAB_4687 and MAB_0314c (Table S1), indicating an ability of these Tn-Seq conditions
170 to identify physiologically relevant antibiotic-response genes.
171
172 To identify other cellular processes necessary for persister survival we performed pathway
173 enrichment analysis on the set of genes identified by Tn-Seq. We used the DAVID[41] analysis tool
174 to perform systematic queries of the KEGG, GO, and Uniprot databases and identify over-
175 represented processes and pathways. Interestingly, although cells were exposed to translation-
176 inhibiting antibiotics, and no exogenous oxidative or nitrosative stress was applied to the cells, we
177 identified a number of factors needed to combat these stresses. This includes *bfrB* (bactoferritin),
178 *ahpe* (peroxiredoxin) and *katG* (catalase/peroxidase) as well as 5 components of the bacterial
179 proteasome pathway, known to mediate resistance to nitrosative stress in *Mtb*[42]. We also
180 identified multiple members of DNA-damage response pathways including *recF*, *recG*, *uvrA*, *uvrB*
181 and *uvrC* (Figure 2G, Table S2). Examining starvation-induced persisters, a number of the same

182 pathways were again seen, and the mutant with the greatest persister defect in this context was
183 *mntH*, a redox-regulated Mn/Zn transporter implicated in peroxide resistance in other organisms[43-
184 44]. Taken together, these findings suggest an unexpected scenario whereby translation inhibition
185 triggers accumulation of reactive oxygen or nitrogen species, with damage to macromolecules
186 such as DNA occurring.
187
188 We next sought to independently confirm a role in persister survival for genes identified by Tn-
189 Seq. We selected a set of genes with strong defects in persister formation, representing several
190 of the functional pathways identified, and used oligonucleotide-mediated recombineering
191 (ORBIT)[45] to disrupt their open reading frames. The initial genes selected were *pafA* (proteasome
192 pathway), *katG* (catalase-peroxidase), *recR* (DNA repair), *blaR* (β-lactam sensing), and
193 *MAB_1456c* (cobalamin synthesis). To control for non-specific effects of antibiotic selection during
194 the recombineering process, we created a control strain using ORBIT to target a non-coding
195 intergenic region downstream of a redundant tRNA gene (*MAB_t5030c*). We then individually
196 screened each of these mutants to determine if they displayed deficits in persister cell formation
197 by exposing cells to TIG/LZD, either in rich 7H9 media or under starvation conditions, as had been
198 done in the pooled Tn-Seq screen. For Δ*katG* we detected clear defects in persister cell survival
199 following 6 days of antibiotic exposure in either rich media or under starvation-induced conditions,
200 corroborating the results of our Tn-Seq analysis (Figure 3A). We observed smaller defects in the
201 Δ*pafA* and Δ*MAB_1456c* mutants (Figure 3B,C), and in *blaR* found no loss of overall viability, but
202 instead observed a delayed resumption of growth after removal of antibiotics (Figure 3D, data not
203 shown).
204 To further confirm the role of *katG* and *pafA,* and exclude off-target effects of recombineering, we
205 performed genetic complementation analysis by restoring a wild-type copy of each gene into the
206 respective Δ*pafA* and Δ*katG* mutants. In each case, we integrated a single copy of the wild-type

207 gene, under the control of its endogenous promoter, into the genome at the L5 *attB* site (hereafter
208 *pafA+, katG+* strains), and constructed isogenic control strains with empty vector integrated at
209 the same site (hereafter *pafA-, katG-* strains). We confirmed expression of the re-introduced copy
210 of each gene by RT-qPCR in the *pafA+*, and *katG+* strains, and found expression within roughly
211 2-fold of endogenous wild-type levels (Figure 4A,D). We then challenged these strains with
212 TIG/LZD as before. In rich media, where the Δ*katG* mutants have a moderate persistence defect,
213 the *katG+* strain had roughly a 50-fold increase in viable cells relative to the *katG-* strain. We then
214 exposed cells to antibiotics under starvation conditions, where the Δ*katG* mutant phenotype is
215 more severe. Under these conditions the *katG-* cells succumbed rapidly between 3d and 10d after
216 antibiotic exposure, with a 1,000-fold decrease in viable cells relative to control cells, whereas the
217 *katG+* strain showed a near-complete restoration of persistence (Figure 4B). We analogously
218 examined complementation of Δ*pafA* mutants, and although the phenotype of the Δ*pafA* mutant
219 is less severe overall than a Δ*katG* mutant, we saw a similar restoration of survival in *pafA+* cells
220 relative to *pafA-* cells (Figure 4E). We next evaluated whether the *pafA-*, and *katG-* strains were
221 overall more sensitive to the growth inhibitory effects of TIG/LZD, or whether they had specific
222 defects in survival above the mean bactericidal concentration. We performed MIC determination
223 for TIG and LZD individually for each strain, comparing the *katG+*/*katG-* and *pafA+/pafA-* strains.
224 We found that that the MICs for each of these strains were unchanged, demonstrating that these
225 mutants were not more readily inhibited by these antibiotics. Instead, they have more rapid
226 kinetics of cell death at bactericidal concentrations, consistent with a specific defect in antibiotic
227 persistence (Figure 4C,F).
228

229 **Reactive oxygen contributes to antibiotic lethality in *Mabs***

230 We next investigated the role of KatG in persister cell cells more broadly. We began by assessing
231 whether *katG* conferred protection from other antibiotics with diverse mechanisms of action,

232 selecting antibiotics that are used clinically for mycobacterial infections. Because *katG*- mutants
233 showed the greatest defects in starvation-induced persistence, we analyzed survival of *katG*+ and
234 *katG*- strains in starvation-adapted cultures exposed to a panel of different antibiotics. Because
235 both TIG and LZD both act by inhibiting translation, we began by exposing cells to either TIG or
236 LZD alone. As expected, the degree of bacterial killing was significantly less with either agent
237 alone than when they are added in combination. Upon exposure to either of these antibiotics the
238 *katG*- cells died more rapidly than *katG*+ cells, though we note that the final proportion of
239 persisters in the population was unchanged in *katG*- cells (Figure 5A). When we exposed cells to
240 rifabutin (RFB), an RNA polymerase inhibitor, we saw a similar effect, with a 100-fold loss of
241 viability in *katG*- cells relative to the *katG*+ cells (Figure 5B). In contrast, when we exposed
242 cultures to either levofloxacin (gyrase inhibitor) or cefoxitin (β-lactam inhibitor of peptidoglycan
243 cross-linking), *katG* had little to no effect on cell viability (Figure 5C-D). Thus, the role of KatG is
244 context-dependent, suggesting that some antibiotics generate oxidative stress that can be
245 ameliorated by KatG catalase/peroxidase activity while others do not.
246
247 The identification of *katG* as essential for persister cells to survive exposure to TIG/LZD suggests
248 that ROS are present and causing damage. Although TIG/LIN are translation inhibitors that do not
249 directly generate ROS we evaluated whether they might nonetheless be triggering ROS
250 accumulation as a secondary effect. We examined ROS levels in *katG*+ *Mabs* using the ROS
251 indicator dye cellROX, that is retained in cells when it becomes oxidized[46]. At baseline, during
252 log-phase growth in rich media < 3% of cells had ROS accumulation (Figure 5E). We saw a
253 moderate increase in ROS accumulation in starved cultures, with roughly 10% of the population
254 cellROX+. However, when starved cultures were exposed to the TIG/LZD we saw a dramatic
255 increase in ROS accumulation with over 30% cellROX+ cells. Taken together, these data indicate
256 that translation inhibition does indeed have unanticipated downstream effects on cellular redox
257 balance, with ROS accumulation that could be contributing to cell death.

258

259 We next tested whether ROS were contributing to cell death by reducing ROS production and
260 assessing the impact on cell viability. A well-established system for studying hypoxia in
261 mycobacteria is the Wayne Model of gradual-onset hypoxia, whereby low-density cultures are
262 inoculated in sealed vessels with minimal headspace. As the culture slowly grows, the soluble O_2
263 is consumed, resulting in the onset of hypoxia over several days, a process that can be monitored
264 by the decolorization of Methylene Blue dye in the media[47]. Under aerobic conditions in rich
265 media, we observed the expected rapid killing of *Mabs* over the first 5 days with the combination
266 of TIG/LZD, with more rapid loss of viability in KatG- cells. However, under hypoxic conditions,
267 where ROS production is suppressed, we saw much slower bacterial killing. Importantly, under
268 hypoxic conditions *katG*- cells no longer had a survival defect relative to *katG*+ cells, supporting
269 the hypothesis that translation-inhibiting antibiotics also cause secondary accumulation of lethal
270 ROS in antibiotic-treated cells that need to be detoxified by KatG (Figure 5F).

271

272 **Incomplete penetrance of *katG* phenotype among *Mabs* strains**

273 Finally, we tested the role of KatG in *Mabs* clinical strains to determine how widely the role of *katG*
274 is conserved among different *Mabs* strains. We obtained 2 clinical isolates of *Mabs*, used ORBIT
275 to disrupt the *katG* locus, and evaluated the ability of these strains to form both spontaneous and
276 starvation-induced persister cells upon exposure to TIG/LZD. For clinical strain-1, the Δ*katG*
277 mutant showed no defects in either condition (Figure 6B). In contrast, for clinical strain-2, *katG*
278 contributed to starvation-induced persistence, as the Δ*katG* mutant rapidly lost viability in a
279 manner similar to the ATCC 19977 reference strain. However, unlike ATCC 19977, this phenotype
280 only manifested in starvation-induced persister cells, and was not seen in the absence of stress
281 (Figure 6C). Thus, the *katG* phenotype displays incomplete penetrance, and the degree of
282 protection it confers falls along a continuum among *Mabs* strains.

283 In summary, the results of these studies point to an important effect of ROS in amplifying the
284 lethality of some antibiotics in *Mabs*. Through genetic analysis we identified a number of ROS
285 detoxification factors, including KatG, as necessary for persisters to remain viable. This suggested
286 that antibiotics might induce an oxidative state in cells, and direct measurement of ROS following
287 antibiotic exposure indicated that this was indeed the case. Further supporting the deleterious
288 effects of ROS in this context, we found that removal of oxygen both slowed bacterial killing and
289 rendered KatG dispensable. Taken together these results suggest that antibiotic lethality is
290 accelerated by toxic ROS accumulation, and persister survival requires active detoxification
291 systems.
292
293 **DISCUSSION:**
294 **Pathways necessary for persister formation in *Mabs.***
295 The phenomenon of bacterial persistence has been recognized for decades, and has been
296 observed in a broad array of bacterial species. Despite this, a unifying mechanism of persister
297 cell formation has not emerged, suggesting that different pathways may play a role in different
298 contexts. A large body of work comes from *E. coli* where toxin-antitoxin systems such as HipBA[15],
299 Lon protease[16,48] and the (p)ppGpp synthase RelA all contribute to the formation of persister
300 cells[49-52]. However, even within this species other mechanisms seem to function, as RelA
301 contributes to persister cell formation following exposure to β-lactams, but not quinolones[53]. In
302 addition, how exactly these pathways maintain cell viability remains unclear. For example, while
303 (p)ppGpp produced by RelA seems to act through Lon protease[16], the critical substrates in this
304 process are note unknown. It is also unclear how mechanisms identified in one bacterial species
305 may relate to the mechanisms in another. *RelA* plays a role in multiple species of bacteria,
306 including *Pseudomonas aeruginosa*[54], *Staphylococcus aureus*[55], and *Mtb*[56]. However, the role of
307 this pathway does not seem to be universal, as deletion of neither *relA* nor *lon* had an effect on
308 persister formation in *Msmeg*[57]. Interestingly, in our Tn-Seq analysis, we did not identify *relA*.

309 However, a prior study of the *Mabs relA* mutant demonstrates that this strain still synthesizes
310 (p)ppGpp[58], suggesting genetic redundancy and a need to disrupt additional genes in a *relA*
311 mutant in order to study the role of (p)ppGpp in *Mabs*.
312
313 **Mechanisms of antibiotic lethality**
314 The mechanisms of bacterial cell death following antibiotic exposure remains somewhat
315 controversial. The most straightforward explanation is that antibiotics kill by directly disrupting the
316 function of their targets. However, more recently it was suggested that antibiotics kill through a
317 final common pathway of lethal ROS generation, leading to oxidative damage of DNA and other
318 macromolecules[59]. Since that time, there have been studies, both supporting[10,19-20] and refuting
319 the role of ROS[21-22] in antibiotic-mediated cell death.
320
321 Our analysis of *Mabs* persister cells provides new insights. The identification of multiple genes
322 involved in ROS detoxification through an unbiased genome-wide screen suggests that ROS also
323 promotes antibiotic lethality in *Mabs*. This idea is further supported by the detection of elevated levels
324 of ROS after exposure to translation inhibitors, and that removal of oxygen slowed antibiotic killing.
325 Taken together, these data strongly support the idea that ROS are a significant contributor to
326 antibiotic lethality in some contexts. These findings are supported by other published studies in
327 mycobacteria. In *Mabs* and *Msmeg,* other groups have also observed reduced antibiotic-mediated
328 killing in hypoxic conditions[10,36]. In *Mtb*, exposure to rifampin also generates ROS[19,60], and *katG*
329 contributes to survival in rifampin-treated cells[19].
330
331 The source of ROS under these conditions is uncertain. In principle, any of several derangements
332 could lead to ROS accumulation. One of the major sources of cellular ROS is oxidative
333 phosphorylation, as hydrogen peroxide, superoxide, and hydroxyl radicals are natural byproducts.
334 Thus, increased ROS generation by oxidative phosphorylation is an attractive hypothesis.

335 Alternatively, particularly under starvation conditions, it is possible that antioxidants and ROS
336 scavengers may become depleted, creating a more oxidizing environment. Our Tn-Seq analysis
337 provides additional insight on this. We noted a small class of Tn mutants that were paradoxically
338 protected from antibiotic lethality (Figure 2B). Prominent among this class of mutants were several
339 independent components of the NADH dehydrogenase complex (Table S1). Also known as
340 Complex I of the electron transport chain, it is one of the key entry points for electrons into the
341 oxidative phosphorylation pathway. The observation that mutants in this complex are protected
342 suggests that decreasing flux through oxidative phosphorylation, with a concomitant decrease in
343 ROS generation, may enhance survival during antibiotic exposure.
344
345 However, antibiotic-induced ROS accumulation is not a universal phenomenon. With some
346 antibiotics we examined in *Mabs,* loss of *katG* had no effect. In addition, ROS detoxification does
347 not always play a protective role, as loss of catalase and peroxidase activities in *E. coli* also had
348 no effect on persister survival[22]. Taken together, this suggests a model in which antibiotics cause
349 direct toxicity by acting on their target, but in addition, some antibiotics, notably transcription
350 inhibitors and translation inhibitors, also appear to have a secondary toxic effect of causing ROS
351 accumulation. How exactly transcription or translation blockade leads to increased ROS levels is
352 currently unclear and will require further investigation, although our data suggest that the electron
353 transport chain might play an important role.
354
355 **Therapeutic implications**
356 *Mabs* infections are particularly challenging to eradicate, with relapse rates over 50%[28]. Our
357 results highlight several bacterial processes such as the bacterial proteasome or ROS
358 detoxification that might be targeted therapeutically to reduce the development or survival of
359 persister cells. Agents targeting these process might not have any intrinsic antimicrobial activity
360 alone, but might act to target the unique physiology of persister cells that develop upon antibiotic

361 exposure. This would represent a new therapeutic class of “persistence inhibitors” that might act
362 synergistically with traditional antibiotics to eliminate the subpopulation of persister cells that
363 would otherwise remain viable despite prolonged antibiotic exposure in *Mabs* and other chronic
364 infections.
365
366 **Limitations**
367 Tn-Seq has inherent drawbacks, including an inability to identify mutants in essential genes, or in
368 cases of genetic redundancy. Thus, there are likely genes needed for antibiotic persistence in
369 *Mabs* that were not identified in this study. In addition, we studied the response to a single class
370 of antibiotic, focusing on the translation inhibitors often used to treat *Mabs* infections, and we
371 studied only spontaneous and starvation-induced persister cells. It is likely that studying other
372 antibiotics, with different mechanisms of action, or different stresses that induce persister cells,
373 would identify additional genes contributing to persister formation and would allow better
374 identification of core survival pathways that might be shared among different forms of stress.
375
376 **MATERIALS AND METHODS**
377 **Key Reagent Table**

Reagent	**Source/Reference**	**Identifier**
***Mabs* ATCC 19977**	ATCC	19977
***Msmeg* MC2 155**	ATCC	700084
***Mtb* Erdman**	ATCC	35801
***Mabs* clinical strains**	Sacramento Department of Public Health	NA
pkm444	Addgene	108319
pkm496	Addgene	109301

pmv306	Ref. 61	
Middlebrook 7H9	BD	271310
Middlebrook 7H10	BD	262710
Glycerol	Invitrogen	15514011
Tween-80	Fisher	BP338-500
Middlebrook OADC	BD	212351
DPBS (-Ca/Mg)	Gibco	14190144
Tyloxapol	Sigma Aldrich	T8761
Methylene blue	Sigma Aldrich	28514
Tigecycline	Chem Impex	29737
Linezolid	Chem Impex	29723
Levofloxacin	Sigma Aldrich	28266
Cefoxitin	Chem Impex	1490
Rifabutin	Cayman Chemical	16468
Rifampin	Sigma Aldrich	R7382
Isoniazid	Supelco	I3377
Ethambutol	Thermo Scientific	J6069506
DMSO	Sigma Aldrich	D2650
Trizol	Invitrogen	15596018
0.1mm zirconia beads	Biospec	11079101z
PureLink RNA Mini Kit	Invitrogen	12183025
Kanamycin	VWR	75856-686
Zeocin	Invivogen	ANTZN1P
Glycine	Fisher Bioreagents	BP381
Sucrose	Sigma Aldrich	S1888

Anhydrotetracycline	Cayman Chemical	10009542
cellROX green	Invitrogen	C10444
Paraformaldehyde	Sigma Aldrich	P6148
DAPI	Sigma Aldrich	D9542
DNAseI	New England Biolabs	M0303
Maxima H minus reverse transcriptase	Thermo Scientific	EP0752
Taq Polymerase	New England Biolabs	M0273
EvaGreen	Biotium	31019

378

379 Bacterial strains and culture conditions:

380 *Mabs* ATCC 19977, clinical *Mabs* strains and *Msmeg* (MC2 155) were grown in BD Middlebrook
381 7H9 media (liquid) or 7H10 media (solid) supplemented with 0.5% glycerol (Sigma) and 0.2%
382 Tween-80 (Fisher) but without any OADC supplementation except for transformations.
383 Sacramento clinical isolates were obtained from the Sacramento County Department of Public
384 Health Mycobacteriology Laboratory. Confirmation of clinical isolates as *Mabs* was performed by
385 amplifying the 16s rRNA locus and Sanger sequencing. *Mtb* (Erdman) was grown in 7H9 (liquid)
386 or 7H10 (solid) supplemented with 0.5% glycerol, 0.1% Tween-80, and 10% OADC (BD). All
387 cultures were grown at 37°C with gentle shaking. Except for specific hypoxia conditions, all liquid
388 cultures were grown with 90% container headspace or using a gas permeable cap to ensure
389 culture oxygenation. PBS starvation was achieved by washing OD0.5-1.0 *Mabs* 1X in DPBS (-
390 Ca/Mg, Gibco) and resuspending in DPBS at OD=1, supplemented with 0.1% tyloxapol (Sigma).

391

392 *Mabs* antibiotic experiments:

393 For PBS starvation experiments, stocks of *Mabs* were grown for 48 hours in 7H9 passaging
394 continuously in log phase, then PBS starved or passaged in log phase for an additional 48h. Log
395 phase or PBS starved *Mabs* were then resuspended in antibiotic containing media at OD1.0. For
396 experiments with hypoxia, *Mabs* in mid-log aerobic growth was adjusted to OD0.001 in media
397 with 1.5ug/ml methylene blue and added to a rubber septum sealed glass vial with 50%
398 headspace. Methylene blue discoloration was observed at 3d and antibiotics were added at 5d.
399 We empirically determined the half-life of each antibiotic in 7H9 media at 37-deg and for those
400 with half-lives shorter than the experiment, supplemented cultures to with additional antibiotic to
401 maintain the concentration of active antibiotic. Antibiotics were used at the following
402 concentrations: tigecycline (Chem-Impex) at 10ug/ml (8 fold above MIC, re-administered every 3
403 days), linezolid (Chem-Impex) at 100ug/ml (20 fold above MIC), levofloxacin (Sigma) at 40ug/ml
404 (8 fold above MIC), cefoxitin (Chem Impex) at 80ug/ml (8 fold above MIC, re-administered every
405 3 days), and rifabutin (Cayman) at 40ug/ml (4 fold above MIC). After antibiotic administration,
406 colony forming units over time were measured.
407
408 *Msmeg* antibiotic experiments:
409 Individual colonies were picked and grown for 48 hours in log phase before being PBS starved or
410 passaged in log phase for 48h. Log phase or PBS starved *Msmeg* were then resuspended in
411 antibiotic containing media at OD1.0. Antibiotics were used at the following concentrations:
412 tigecycline (Chem-Impex) at 1.25ug/ml (8 fold above MIC, re-administered every 3 days), linezolid
413 (Chem-Impex) at 2.5ug/ml (8 fold above MIC), rifampin (Sigma) at 32ug/ml (8 fold above MIC, re-
414 administered every 6 days), isoniazid (Sigma) at 32ug/ml (8 fold above MIC, re-administered
415 every 6 days), and ethambutol (Thermo) at 4ug/ml (8 fold above MIC, re-administered every 3
416 days). After antibiotic administration, colony forming units over time were measured.
417
418 *Mtb* antibiotic experiments:

419 Freezer stocks of *Mtb* were thawed and grown for 5-7 days in log phase before being starved for
420 14d or longer. Non-starved control *Mtb* were thawed such that they were also grown for 5-7 days
421 in log phase before experimental use. Log phase or PBS starved *Mtb* was then resuspended in
422 antibiotic containing media and adjusted to OD1.0. Antibiotics were used at the following
423 concentrations: rifampin (Sigma) at 0.1ug/ml (4 fold above MIC, re-administered every 6 days),
424 isoniazid (Sigma) at 0.1ug/ml (4 fold above MIC, re-administered every 6 days), and ethambutol
425 (Thermo) at 8ug/ml (4 fold above MIC, re-administered every 6 days). After antibiotic
426 administration, colony forming units over time were measured.
427
428 Transposon insertion sequencing:
429 The construction of this *Himar1* transposon Tn library has been described previously [29]. Screening
430 was performed by growing a freezer stock of the library for 2.5 days in log phase before 48-hour
431 PBS starvation or further continuous log-phase growth. Samples were then resuspended in media
432 containing either tigecycline/linezolid or an equal volume of DMSO solvent and incubated for 6
433 days, with a re-administration of tigecycline or matching DMSO on day 3. The samples were then
434 washed 2X in antibiotic free liquid media, resuspended in antibiotic free liquid media (10X the
435 original culture volume), and grown until OD0.5-1.0. Subsequently, the samples underwent three
436 more rounds of 100-fold passaging in liquid media to amplify surviving bacteria before the
437 samples were collected in Trizol (Invitrogen). A sample taken at the time of the commencement
438 of PBS starvation was collected in Trizol and used as the input control. Three independent trials
439 of this experiment were submitted to the UC Davis DNA Technologies Core, where Tn insertion
440 site flanking sequences were amplified as described previously [29] and sequenced on sequenced
441 on an Illumina AVITI. Sequence reads were mapped to the ATCC 19977 genome and analyzed
442 using TRANSIT software with the following parameters: 0% of N/C termini ignored, 10,000
443 samples, TTR normalization, LOESS correction, include sites with all zeros, site restricted

444 resampling. Genes with significant changes were defined as those with adjusted p-value (p-adj.)
445 <0.05 and $\log_2$ fold change >0.5. P-adj. was calculated using the Benjamini-Hochberg correction.
446
447 Pathway enrichment analysis
448 To improve gene annotation, *Mabs* orthologs to *Mtb* genes were identified. *Mabs* genes were first
449 converted into protein sequences using Mycobrowser, and protein sequences were then used to
450 perform reciprocal BLASTp searches. *Mabs* genes and *Mtb* genes that mapped to each other
451 using independent one-way BLASTp searches with a maximum e-value cutoff of 0.1 were
452 considered orthologs. For pathway analysis, gene lists (*Mtb* orthologs) were then imported into
453 the DAVID knowledgebase[41] and pathway enrichment analysis performed for Gene Ontology
454 biological process, Uniprot keyword and KEGG databases with statistical analysis Fisher's exact
455 test and nominal p-value reported.
456
457 Gene deletion and complementation:
458 Knockout strains were generated using ORBIT[45]. Briefly, *Mabs* was transformed with the
459 kanamycin-resistant ORBIT recombineering plasmid pkm444. 20ml *Mabs* at OD0.5-1.0 was
460 washed 2X in 10% glycerol and resuspended in 200ul 10% glycerol. 500ng plasmid was added
461 and electroporated at 2.5kV in 0.2cm cuvettes. The bacteria were allowed to recover overnight
462 before plating on 150ug/ml kanamycin plates. Clones were selected and regrown in liquid media
463 supplemented with 150ug/ml kanamycin and 10% OADC (BD) to OD0.5-1.0. For recombineering,
464 the pkm444-*Mabs* was grown to mid-log, then diluted to OD0.1 and 200mM glycine (Fisher) was
465 added to the media. 16 hours later, 500mM sucrose (Sigma) and 500ng/ml anhydrotetracycline
466 (Cayman) were added and incubated for an additional 4 hours. Subsequently, the *Mabs* was
467 washed 2X in ice cold 10% glycerol + 500mM sucrose. 200ul of 10X concentrated *Mabs* was then
468 electroporated with 600ng of the zeocin-R ORBIT payload pkm496 plasmid and 2ug of targeting
469 oligonucleotide (Table S3) at 2.5kV in 0.2cm cuvettes. The *Mabs* was then allowed to recover

470 overnight in liquid media with 10% OADC and 500ng/ml anhydrotetracycline before being plated
471 on 150ug/ml zeocin plates. Mutants were then selected and screened for gene deletion by PCR
472 amplification and Sanger sequencing. For genetic complementation, the endogenous loci
473 including promoter and terminator sequences were amplified by PCR and cloned into the EcoRV
474 site of pmv306 with kanamycin resistance[61]. In the case of *katG,* the upstream gene *furA* was
475 also included in the complementation construct to achieve optimal *katG* expression.
476
477 MIC analysis
478 Two-fold serial dilutions of antibiotics were prepared in a 96 well plate in 100ul volume. 100ul of
479 2X bacteria were added (for *Mabs*: used a final OD of 0.001, *Msmeg*: OD0.001, *Mtb*: OD0.01),
480 making a final volume of 200ul. The plates were incubated until there was visible growth in the no
481 antibiotic control well. At this time, the bacteria were transferred to a new plate with 20ul of 40%
482 paraformaldehyde and OD620 measurements were taken with a FilterMax F3 plate reader
483 (Molecular Devices).
484
485 Flow cytometry
486 OD1 Mab was stained with cellROX green (Invitrogen) at a final concentration of 5uM for 1hr at
487 37C. The cells were then washed in PBS and resuspended in PBS with 4% paraformaldehyde
488 and 5ug/ml DAPI (Sigma). The samples were run on a LSRII flow cytometer (BD). Fluorophores
489 were excited with the 405nm (DAPI) and 488nm (cellROX) lasers. Detection was performed using
490 the 450/50 (505LP) filter for DAPI and a 525/50 (555LP) filter for cellROX. Data were analyzed
491 with FlowJo software (BD).
492
493
494 DNA/RNA Purification:

495 Samples were resuspended in 5 volumes of Trizol and were bead beat with 0.1mm zirconia beads
496 (Biospec) 6x2min at 4°C in a Mini-Beadbeater-16 (Biospec). Chloroform was added and RNA in
497 the aqueous phase removed. For DNA isolation, a second RNA extraction was performed with
498 0.8M guanidine thiocyanate and 0.5M guanidine hydrochloride, 60mM Acetate pH 5.2, 1mM
499 EDTA. DNA was then isolated with back-extraction buffer (4M Guanidine Thiocyanate, 50mM
500 Sodium Citrate, 1M Tris base (without pH adjustment ~pH 11) and DNA purified using a PureLink
501 RNA Mini Kit (Invitrogen).
502
503 RT-qPCR
504 RNA was purified using PureLink RNA Mini Kit per manufacturer's instructions. The samples were
505 DNAseI (NEB) treated for 15min/37°C before stopping the reaction by adding 3.5mM EDTA and
506 heating for 10min/75°C. cDNA was synthesized from 500ng total RNA using random hexamers
507 and Maxima H minus reverse transcriptase (Thermo). No reverse-transcription controls were also
508 included and used to confirm the lack of genomic DNA-driven amplification. qPCR reactions used
509 Taq polymerase (NEB) and EvaGreen (Biotium) and were run on Biorad CFX Opus 96 Real-Time
510 PCR System. Melt curves were included for each sample to confirm uniform amplicon identity
511 between samples. Gene-specific amplification was quantified by comparison to a standard curve
512 generated from 3-fold serial dilutions of a control sample, then normalized to 16S rRNA within
513 each sample.
514
515 **FIGURE LEGENDS**
516 **Figure 1. Starvation induces antibiotic persister cells across diverse mycobacteria.** (A)
517 *Msmeg,* (B) *Mtb* or (C) *Mabs* were grown in 7H9 rich media or starved in PBS prior to the addition
518 of the indicated antibiotics. Cells were allowed to adapt to starvation for a period of 48h for *Msmeg*
519 and *Mabs* and 14-21d for *Mtb* prior to the addition of antibiotics in PBS where indicated. (D-F) As
520 above, but with/without a period of adaptation in PBS prior to antibiotics as indicated. Antibiotic

521 concentrations were: *Msmeg* - Isoniazid (INH) 32ug/ml (8 x MIC), rifampin (RIF) 32ug/ml (8 x
522 MIC), ethambutol (EMB) 4ug/ml (8 x MIC), tigecycline (TIG) 1.25ug/ml (8 x MIC), linezolid (LZD)
523 2.5ug/ml (8 x MIC). *Mtb* – RIF 0.1ug/ml (4 x MIC), INH at 0.1ug/ml (4 x MIC), EMB at 8ug/ml (4 x
524 MIC). *Mabs* – TIG (8 x MIC), LZD 100ug/ml (20 x MIC). Antibiotics with half-lives shorter than the
525 duration of experiment were re-added at the following intervals: TIG, EMB every 3d; RIF, INH
526 every 6d. Error bars represent SEM, statistical significance is calculated at each time point using
527 student's t test. ****: $p<0.0001$, ***: $p<0.001$, **: $p<0.01$, *: $p<0.05$, ns: $p>0.05$. Data are combined
528 from 3 independent experiments.
529
530 **Figure 2. Tn-Seq identifies genes required for antibiotic persistence in *Mabs*.** (A)
531 Experimental design. (B-E) Tn-Seq analysis showing relative abundance of individual genes
532 under the indicted conditions. All cultures were fully aerated throughout the experiment and
533 cultures without antibiotics received and equal volume of DMSO. For (B-D) gene abundance in
534 the indicated condition is measured relative the input log-phase population. In (E) an additional
535 comparison is made relative to the PBS condition. Genes with significant decreases in abundance
536 are shown in color (p-adj. < 0.05 and $\log_2$ fold-change > 0.5) using the Benjamini–Hochberg
537 adjustment for multiple hypothesis testing. (F) Number of genes essential in each condition
538 relative to the input population. (G) Pathway enrichment analysis of the essential genes in each
539 condition using the DAVID knowledgebase ($p <0.05$). Screens were run as 3 independent
540 experiments and the combined results analyzed. Antibiotic conditions were used as described in
541 Figure 1.
542
543 **Figure 3. Independent deletions of *katG* and *pafA* confirm Tn-Seq results.** (A-E) ORBIT
544 recombineering was used to disrupt the indicated genes, or to generate a control strain with an
545 intergenic region targeted distal to tRNA gene *MAB_t5030c*. Each mutant was either grown in
546 7H9 rich media or starved in PBS for 48 prior to the addition of antibiotics. Error bars represent

547 SEM, statistical significance is calculated at each time point using student's t test. ****: p<0.0001,
548 ***: p<0.001, **: p<0.01, *: p<0.05, ns: p>0.05. Antibiotics were added as described above. Data
549 are combined from 4 independent experiments.
550
551 **Figure 4. Complementation analysis *katG* and *pafA* mutants confirms their role in persister**
552 **survival.** (A) RT-qPCR analysis of *katG* expression in *katG- (Δ katG::pmv306), katG+*
553 *(Δ katG::pmv306 katG),* and control strain (ORBIT intergenic*::pmv306).* (B) CFU over time for
554 *katG+/katG-* strains. (C) MICs for *katG+/katG-* strains. (D) Expression of *pafA in pafA-*
555 *(Δ pafA::pmv306), pafA+ (pafA::pmv306 pafA)* and control strains. (E) CFU over time of
556 *pafA+/pafA-* strains. (F) MICs for *pafA+/pafA-* strains. Antibiotic concentrations in (A-B, D-E) are
557 as described above. Error bars represent SEM, statistical significance is calculated at each time
558 point using student's t test between *katG+/katG-* strains in (B) and between *pafA+/pafA-* strains
559 in (E). ****: p<0.0001, ***: p<0.001, **: p<0.01, *: p<0.05, ns: p>0.05. Antibiotics were added as
560 described above.
561
562 **Figure 5. ROS-mediated toxicity following antibiotic exposure.** (A-D) Analysis of *katG+/katG-*
563 cells challenged with different antibiotics. Cells were starved in PBS for 48h and then exposed to
564 the indicated antibiotic. (E) Flow cytometry of cells *katG*$^{+}$ cells stained with DAPI and the ROS-
565 sensitive dye cellROX after 72h in the indicated conditions. Percentage cellROX-positive cells are
566 shown. (F) Persister survival over time for aerated and hypoxic and cultures of *Mabs* after
567 exposure to TIG/LIN. Error bars represent SEM, statistical significance is calculated at each time
568 point using student's t test. ****: p<0.0001, ***: p<0.001, **: p<0.01, *: p<0.05, ns: p>0.05. (A-D)
569 are combined data from 3 independent experiments. (E) are representative (median) data from 3
570 independent experiments. (F) are combined data from 4 independent experiments. Antibiotics
571 were added as described above.

572

573 **Figure 6. Incomplete penetrance of *katG* phenotype among *Mabs* strains.** Δ*katG* strains and
574 control strains targeting an intergenic region were constructed on the indicated *Mabs*
575 backgrounds using ORBIT recombineering: (A) ATCC 19977, (B-C) clinical strains. Bacteria were
576 cultured in 7H9 or starved for 48h in PBS and then treated with antibiotics where indicated.
577 Cultures without antibiotics received an equal volume of DMSO as a control. Survival over time
578 is shown. Error bars represent SEM, statistical significance is calculated at each time point using
579 student's t test. ****: $p<0.0001$, ***: $p<0.001$, **: $p<0.01$, *: $p<0.05$, ns: $p>0.05$.Combined data
580 from 4 independent experiments are shown. Antibiotics were added as described above.

581

582 **Table S1. Tn-Seq results**

583 **Table S2. DAVID functional pathway analysis**

584 **Table S3. Oligonucleotide sequences**

585

586 **ACKNOWLEDGEMENTS**

587 We would like to thank Nick Campbell-Kruger for his technical insights on identifying *Mabs/Mtb*
588 orthologs, Jonathan Van Dyke for his assistance with flow cytometry analysis, Emily Kumimoto
589 and Siranoosh Ashtari for their assistance with Tn-Seq library preparation and sequencing, and
590 Jessie Li and Bradley Jenner for their assistance with Tn-seq bioinformatics. We would also like
591 to thank Caroline Dominic at the Sacramento County Department of Public Health for providing
592 clinical isolates of *Mabs* for analysis.

593

594 **FUNDING**

595 Pew Biomedical Fellowship BHP

596 NIH RO1 1R01AI144149 BHP

597 NIH R01 1R01AI143722 SAS

598 NIH Shared Instrumentation Grant 1S10OD010786-01 DNA Technologies and Expression
599 Analysis Core, UC Davis Genome Center
600 NCI Cancer Center Support Grant P30CA093373 Flow Cytometry Shared Resource, UC Davis
601

602 **CONFLICTS OF INTEREST**

603 BHP and SAS serve on the scientific advisory board of X-Biotics Therapeutics.

604

605 **REFERENCES**

606 1. Stevens, D.L., A.L. Bisno, H.F. Chambers, E.P. Dellinger, E.J. Goldstein, S.L. Gorbach,
607 J.V. Hirschmann, S.L. Kaplan, J.G. Montoya, and J.C. Wade, *Practice guidelines for the*
608 *diagnosis and management of skin and soft tissue infections: 2014 update by the*
609 *Infectious Diseases Society of America.* Clin Infect Dis, 2014. **59**(2): p. e10-52.
610 2. Metersky, M.L. and A.C. Kalil, *Management of ventilator-associated pneumonia:*
611 *guidelines.* Clinics in chest medicine, 2018. **39**(4): p. 797-808.
612 3. Meylan, S., I.W. Andrews, and J.J. Collins, *Targeting Antibiotic Tolerance, Pathogen by*
613 *Pathogen.* Cell, 2018. **172**(6): p. 1228-1238.
614 4. Namugenyi, S.B., A.M. Aagesen, S.R. Elliott, and A.D. Tischler, *Mycobacterium*
615 *tuberculosis PhoY Proteins Promote Persister Formation by Mediating Pst/SenX3-*
616 *RegX3 Phosphate Sensing.* mBio, 2017. **8**(4): p. e00494-17.
617 5. Liu, Y., S. Tan, L. Huang, R.B. Abramovitch, K.H. Rohde, M.D. Zimmerman, C. Chen, V.
618 Dartois, B.C. VanderVen, and D.G. Russell, *Immune activation of the host cell induces*
619 *drug tolerance in Mycobacterium tuberculosis both in vitro and in vivo.* Journal of
620 Experimental Medicine, 2016. **213**(5): p. 809-825.
621 6. Gold, B. and C. Nathan, *Targeting Phenotypically Tolerant Mycobacterium tuberculosis.*
622 Microbiol Spectr, 2017. **5**(1).

623 7. Bigger, J.J.T.L., *Treatment of staphylococcal infections with penicillin by intermittent*
624 *sterilisation.* 1944. **244**(6320): p. 497-500.
625 8. Ronneau, S., P.W.S. Hill, and S. Helaine, *Antibiotic persistence and tolerance: not just*
626 *one and the same.* Current opinion in microbiology, 2021. **64**: p. 76-81.
627 9. Dhar, N. and J.D. McKinney, *Microbial phenotypic heterogeneity and antibiotic tolerance.*
628 Current opinion in microbiology, 2007. **10**(1): p. 30-38.
629 10. Grant, S.S., B.B. Kaufmann, N.S. Chand, N. Haseley, and D.T. ng, *Eradication of*
630 *bacterial persisters with antibiotic-generated hydroxyl radicals.* Proceedings of the
631 National Academy of Sciences, 2012. **109**(30): p. 12147-12152.
632 11. Baker, J.J. and R.B. Abramovitch, *Genetic and metabolic regulation of Mycobacterium*
633 *tuberculosis acid growth arrest.* Scientific Reports, 2018. **8**(1).
634 12. Saito, K., T. Warrier, S. Somersan-Karakaya, L. Kaminski, J. Mi, X. Jiang, S. Park, K.
635 Shigyo, B. Gold, and J. Roberts, *Rifamycin action on RNA polymerase in antibiotic-*
636 *tolerant Mycobacterium tuberculosis results in differentially detectable populations.*
637 Proceedings of the National Academy of Sciences, 2017. **114**(24): p. E4832-E4840.
638 13. Hipolito, V.E.B., E. Ospina-Escobar, and R.J. Botelho, *Lysosome remodelling and*
639 *adaptation during phagocyte activation.* Cell Microbiol, 2018. **20**(4).
640 14. Sukumar, N., S. Tan, B.B. Aldridge, and D.G. Russell, *Exploitation of Mycobacterium*
641 *tuberculosis reporter strains to probe the impact of vaccination at sites of infection.* PLoS
642 Pathog, 2014. **10**(9): p. e1004394.
643 15. Schumacher, M.A., K.M. Piro, W. Xu, S. Hansen, K. Lewis, and R.G. Brennan, *Molecular*
644 *Mechanisms of HipA-Mediated Multidrug Tolerance and Its Neutralization by HipB.*
645 Science, 2009. **323**(5912): p. 396-401.
646 16. Harms, A., C. Fino, A. Sørensen Michael, S. Semsey, and K. Gerdes, *Prophages and*
647 *Growth Dynamics Confound Experimental Results with Antibiotic-Tolerant Persister*
648 *Cells.* mBio, 2017. **8**(6): p. 10.1128/mbio.01964-17.

649 17. Korch, S.B., T.A. Henderson, and T.M. Hill, *Characterization of the hipA7 allele of*
650 *Escherichia coli and evidence that high persistence is governed by (p)ppGpp synthesis.*
651 Mol Microbiol, 2003. **50**(4): p. 1199-213.
652 18. Wong, F., S. Wilson, R. Helbig, S. Hegde, O. Aftenieva, H. Zheng, C. Liu, T. Pilizota, E.C.
653 Garner, A. Amir, and L.D. Renner, *Understanding Beta-Lactam-Induced Lysis at the*
654 *Single-Cell Level.* Frontiers in Microbiology, 2021. **12**.
655 19. Saito, K., S. Mishra, T. Warrier, N. Cicchetti, J. Mi, E. Weber, X. Jiang, J. Roberts, A.
656 Gouzy, E. Kaplan, C.D. Brown, B. Gold, and C. Nathan, *Oxidative damage and delayed*
657 *replication allow viable Mycobacterium tuberculosis to go undetected.* Sci Transl Med,
658 2021. **13**(621): p. eabg2612.
659 20. Vilchèze, C., T. Hartman, B. Weinrick, P. Jain, T.R. Weisbrod, L.W. Leung, J.S.
660 Freundlich, and W.R. Jacobs, Jr., *Enhanced respiration prevents drug tolerance and*
661 *drug resistance in Mycobacterium tuberculosis.* Proc Natl Acad Sci U S A, 2017. **114**(17):
662 p. 4495-4500.
663 21. Keren, I., S. Minami, E. Rubin, and K. Lewis, *Characterization and transcriptome*
664 *analysis of Mycobacterium tuberculosis persisters.* mBio, 2011. **2**(3): p. e00100-11.
665 22. Liu, Y. and J.A. Imlay, *Cell death from antibiotics without the involvement of reactive*
666 *oxygen species.* Science, 2013. **339**(6124): p. 1210-3.
667 23. de Keijzer, J., A. Mulder, J. de Beer, A.H. de Ru, P.A. van Veelen, and D. van Soolingen,
668 *Mechanisms of Phenotypic Rifampicin Tolerance in Mycobacterium tuberculosis Beijing*
669 *Genotype Strain B0/W148 Revealed by Proteomics.* J Proteome Res, 2016. **15**(4): p.
670 1194-204.
671 24. Gold, B., T. Warrier, and C. Nathan, *A multi-stress model for high throughput screening*
672 *against non-replicating Mycobacterium tuberculosis.* Mycobacteria protocols, 2015: p.
673 293-315.

674 25. Dorman, S.E., P. Nahid, E.V. Kurbatova, P.P. Phillips, K. Bryant, K.E. Dooley, M. Engle,
675 S.V. Goldberg, H.T. Phan, and J. Hakim, *Four-month rifapentine regimens with or without*
676 *moxifloxacin for tuberculosis.* New England Journal of Medicine, 2021. **384**(18): p. 1705-
677 1718.
678 26. Nahid, P., S.E. Dorman, N. Alipanah, P.M. Barry, J.L. Brozek, A. Cattamanchi, L.H.
679 Chaisson, R.E. Chaisson, C.L. Daley, and M. Grzemska, *Official American thoracic*
680 *society/centers for disease control and prevention/infectious diseases society of America*
681 *clinical practice guidelines: treatment of drug-susceptible tuberculosis.* Clinical infectious
682 diseases, 2016. **63**(7): p. e147-e195.
683 27. Griffith, D.E., T. Aksamit, B.A. Brown-Elliott, A. Catanzaro, C. Daley, F. Gordin, S.M.
684 Holland, R. Horsburgh, G. Huitt, and M.F. Iademarco, *An official ATS/IDSA statement:*
685 *diagnosis, treatment, and prevention of nontuberculous mycobacterial diseases.*
686 American journal of respiratory and critical care medicine, 2007. **175**(4): p. 367-416.
687 28. Griffith, D.E. and C.L. Daley, *Treatment of Mycobacterium abscessus Pulmonary*
688 *Disease.* CHEST, 2022. **161**(1): p. 64-75.
689 29. Rodriguez, R., N. Campbell-Kruger, J. Gonzalez Camba, J. Berude, R. Fetterman, and
690 S. Stanley, *MarR-Dependent Transcriptional Regulation of mmpSL5 Induces*
691 *Ethionamide Resistance in Mycobacterium abscessus.* Antimicrobial Agents and
692 Chemotherapy, 2023. **67**(4): p. e01350-22.
693 30. Li, S., N.C. Poulton, J.S. Chang, Z.A. Azadian, M.A. DeJesus, N. Ruecker, M.D.
694 Zimmerman, K.A. Eckartt, B. Bosch, C.A. Engelhart, D.F. Sullivan, M. Gengenbacher,
695 V.A. Dartois, D. Schnappinger, and J.M. Rock, *CRISPRi chemical genetics and*
696 *comparative genomics identify genes mediating drug potency in Mycobacterium*
697 *tuberculosis.* Nature microbiology, 2022. **7**(6): p. 766-779.
698 31. Carey, A.F., J.M. Rock, I.V. Krieger, M.R. Chase, M. Fernandez-Suarez, S. Gagneux,
699 J.C. Sacchettini, T.R. Ioerger, and S.M. Fortune, *TnSeq of Mycobacterium tuberculosis*

700 *clinical isolates reveals strain-specific antibiotic liabilities.* PLoS pathogens, 2018. **14**(3):
701 p. e1006939.
702 32. Kreutzfeldt, K.M., R.S. Jansen, T.E. Hartman, A. Gouzy, R. Wang, I.V. Krieger, M.D.
703 Zimmerman, M. Gengenbacher, J.P. Sarathy, M. Xie, V. Dartois, J.C. Sacchettini, K.Y.
704 Rhee, D. Schnappinger, and S. Ehrt, *CinA mediates multidrug tolerance in*
705 *Mycobacterium tuberculosis.* Nat Commun, 2022. **13**(1): p. 2203.
706 33. Block, A.M., S.B. Namugenyi, N.P. Palani, A.M. Brokaw, L. Zhang, K.B. Beckman, and
707 A.D. Tischler, *Mycobacterium tuberculosis Requires the Outer Membrane Lipid*
708 *Phthiocerol Dimycocerosate for Starvation-Induced Antibiotic Tolerance.* Msystems,
709 2023. **8**(1): p. e0069922.
710 34. Bellerose, M.M., S.-H. Baek, C.-C. Huang, C.E. Moss, E.-I. Koh, M.K. Proulx, C.M.
711 Smith, R.E. Baker, J.S. Lee, S. Eum, S.J. Shin, S.-N. Cho, M. Murray, and C.M. Sassetti,
712 *Common Variants in the Glycerol Kinase Gene Reduce Tuberculosis Drug Efficacy.*
713 mBio, 2019. **10**(4): p. e00663-19.
714 35. Kumar, K., C.L. Daley, D.E. Griffith, and M.R. Loebinger, *Management of Mycobacterium*
715 *avium complex and Mycobacterium abscessus pulmonary disease: therapeutic*
716 *advances and emerging treatments.* European respiratory review, 2022. **31**(163).
717 36. Yam, Y.K., N. Alvarez, M.L. Go, and T. Dick, *Extreme Drug Tolerance of Mycobacterium*
718 *abscessus "Persisters".* Front Microbiol, 2020. **11**: p. 359.
719 37. Berube, B.J., L. Castro, D. Russell, Y. Ovechkina, and T. Parish, *Novel Screen to Assess*
720 *Bactericidal Activity of Compounds Against Non-replicating Mycobacterium abscessus.*
721 Front Microbiol, 2018. **9**: p. 2417.
722 38. Lee, J., N. Ammerman, A. Agarwal, M. Naji, S.Y. Li, and E. Nuermberger, *Differential In*
723 *Vitro Activities of Individual Drugs and Bedaquiline-Rifabutin Combinations against*
724 *Actively Multiplying and Nutrient-Starved Mycobacterium abscessus.* Antimicrob Agents
725 Chemother, 2021. **65**(2).

726 39. Betts, J.C., P.T. Lukey, L.C. Robb, R.A. McAdam, and K. Duncan, *Evaluation of a*
727 *nutrient starvation model of Mycobacterium tuberculosis persistence by gene and protein*
728 *expression profiling.* Molecular Microbiology, 2002. **43**(3): p. 717-731.
729 40. DeJesus, M.A., C. Ambadipudi, R. Baker, C. Sassetti, and T.R. Ioerger, *TRANSIT-a*
730 *software tool for Himar1 TnSeq analysis.* PLoS computational biology, 2015. **11**(10): p.
731 e1004401.
732 41. Huang da, W., B.T. Sherman, and R.A. Lempicki, *Systematic and integrative analysis of*
733 *large gene lists using DAVID bioinformatics resources.* Nat Protoc, 2009. **4**(1): p. 44-57.
734 42. Darwin, K.H., S. Ehrt, J.-C. Gutierrez-Ramos, N. Weich, and C.F. Nathan, *The*
735 *proteasome of Mycobacterium tuberculosis is required for resistance to nitric oxide.*
736 Science, 2003. **302**(5652): p. 1963-1966.
737 43. Shi, H., R. Zhang, L. Lan, Z. Chen, and J. Kan, *Zinc mediates resuscitation of lactic acid-*
738 *injured Escherichia coli by relieving oxidative stress.* Journal of Applied Microbiology,
739 2019. **127**(6): p. 1741-1750.
740 44. Hohle, T.H. and M.R. O'Brian, *The mntH gene encodes the major Mn(2+) transporter in*
741 *Bradyrhizobium japonicum and is regulated by manganese via the Fur protein.* Mol
742 Microbiol, 2009. **72**(2): p. 399-409.
743 45. Murphy, K.C., S.J. Nelson, S. Nambi, K. Papavinasasundaram, C.E. Baer, and C.M.
744 Sassetti, *ORBIT: a new paradigm for genetic engineering of mycobacterial*
745 *chromosomes.* mBio, 2018. **9**(6): p. e01467-18.
746 46. McBee, M.E., Y.H. Chionh, M.L. Sharaf, P. Ho, M.W.L. Cai, and P.C. Dedon, *Production*
747 *of superoxide in bacteria is stress- and cell state-dependent: A gating-optimized flow*
748 *cytometry method that minimizes ROS measurement artifacts with fluorescent dyes.*
749 Frontiers in Microbiology, 2017. **8**(MAR).

750 47. Wayne, L.G. and L.G. Hayes, *An In Vitro Model for Sequential Study of Shiftdown of*
751 *Mycobacterium tuberculosis through Two Stages of Nonreplicating Persistence.* Infection
752 and Immunity, 1996. **64**(6): p. 2062-2069.
753 48. Brazas Michelle, D., B.M. Breidenstein Elena, J. Overhage, and E.W. Hancock Robert,
754 *Role of Lon, an ATP-Dependent Protease Homolog, in Resistance of Pseudomonas*
755 *aeruginosa to Ciprofloxacin.* Antimicrobial Agents and Chemotherapy, 2007. **51**(12): p.
756 4276-4283.
757 49. Kusser, W. and E.E. Ishiguro, *Involvement of the relA gene in the autolysis of*
758 *Escherichia coli induced by inhibitors of peptidoglycan biosynthesis.* Journal of
759 Bacteriology, 1985. **164**(2): p. 861-865.
760 50. Bokinsky, G., E.E.K. Baidoo, S. Akella, H. Burd, D. Weaver, J. Alonso-Gutierrez, H.
761 García-Martín, T.S. Lee, and J.D. Keasling, *HipA-Triggered Growth Arrest and β-Lactam*
762 *Tolerance in Escherichia coli Are Mediated by RelA-Dependent ppGpp Synthesis.*
763 Journal of Bacteriology, 2013. **195**(14): p. 3173-3182.
764 51. Honsa, E.S., V.S. Cooper, M.N. Mhaissen, M. Frank, J. Shaker, A. Iverson, J. Rubnitz,
765 R.T. Hayden, R.E. Lee, C.O. Rock, E.I. Tuomanen, J. Wolf, and J.W. Rosch, *RelA*
766 *Mutant Enterococcus faecium with Multiantibiotic Tolerance Arising in an*
767 *Immunocompromised Host.* mBio, 2017. **8**(1): p. e02124-16.
768 52. Nguyen, D., A. Joshi-Datar, F. Lepine, E. Bauerle, O. Olakanmi, K. Beer, G. McKay, R.
769 Siehnel, J. Schafhauser, Y. Wang, B.E. Britigan, and P.K. Singh, *Active starvation*
770 *responses mediate antibiotic tolerance in biofilms and nutrient-limited bacteria.* Science,
771 2011. **334**(6058): p. 982-6.
772 53. Kudrin, P., V. Varik, S.R.A. Oliveira, J. Beljantseva, T.D.P. Santos, I. Dzhygyr, D. Rejman,
773 F. Cava, T. Tenson, and V. Hauryliuk, *Subinhibitory Concentrations of Bacteriostatic*
774 *Antibiotics Induce relA-Dependent and relA-Independent Tolerance to*

775 *β-Lactams.* Antimicrobial Agents and Chemotherapy, 2017. **61**(4): p.
776 10.1128/aac.02173-16.
777 54. Viducic, D., T. Ono, K. Murakami, H. Susilowati, S. Kayama, K. Hirota, and Y. Miyake,
778 *Functional analysis of spoT, relA and dksA genes on quinolone tolerance in*
779 *Pseudomonas aeruginosa under nongrowing condition.* Microbiol Immunol, 2006. **50**(4):
780 p. 349-57.
781 55. Geiger, T., B. Kästle, F.L. Gratani, C. Goerke, and C. Wolz, *Two small (p)ppGpp*
782 *synthases in Staphylococcus aureus mediate tolerance against cell envelope stress*
783 *conditions.* J Bacteriol, 2014. **196**(4): p. 894-902.
784 56. Dutta, N.K., L.G. Klinkenberg, M.J. Vazquez, D. Segura-Carro, G. Colmenarejo, F.
785 Ramon, B. Rodriguez-Miquel, L. Mata-Cantero, E. Porras-De Francisco, Y.M. Chuang,
786 H. Rubin, J.J. Lee, H. Eoh, J.S. Bader, E. Perez-Herran, A. Mendoza-Losana, and P.C.
787 Karakousis, *Inhibiting the stringent response blocks Mycobacterium tuberculosis entry*
788 *into quiescence and reduces persistence.* Sci Adv, 2019. **5**(3): p. eaav2104.
789 57. Bhaskar, A., C. De Piano, E. Gelman, J.D. McKinney, and N. Dhar, *Elucidating the role*
790 *of (p) ppGpp in mycobacterial persistence against antibiotics.* IUBMB life, 2018. **70**(9): p.
791 836-844.
792 58. Hunt-Serracín, A.C., M.I. Kazi, J.M. Boll, and C.C. Boutte, *In Mycobacterium abscessus,*
793 *the Stringent Factor Rel Regulates Metabolism but Is Not the Only (p)ppGpp Synthase.*
794 J Bacteriol, 2022. **204**(2): p. e0043421.
795 59. Kohanski, M.A., D.J. Dwyer, B. Hayete, C.A. Lawrence, and J.J. Collins, *A common*
796 *mechanism of cellular death induced by bactericidal antibiotics.* Cell, 2007. **130**(5): p.
797 797-810.
798 60. Sebastian, J., S. Swaminath, R.R. Nair, K. Jakkala, A. Pradhan, and P. Ajitkumar, *De*
799 *Novo Emergence of Genetically Resistant Mutants of Mycobacterium tuberculosis from*

800 *the Persistence Phase Cells Formed against Antituberculosis Drugs In Vitro.* Antimicrob
801 Agents Chemother, 2017. **61**(2).
802 61. Snapper, S.B., L. Lugosi, A. Jekkel, R.E. Melton, T. Kieser, B.R. Bloom, and W.R.
803 Jacobs, Jr., *Lysogeny and transformation in mycobacteria: stable expression of foreign*
804 *genes.* Proc Natl Acad Sci U S A, 1988. **85**(18): p. 6987-91.

805

FIGURE 1

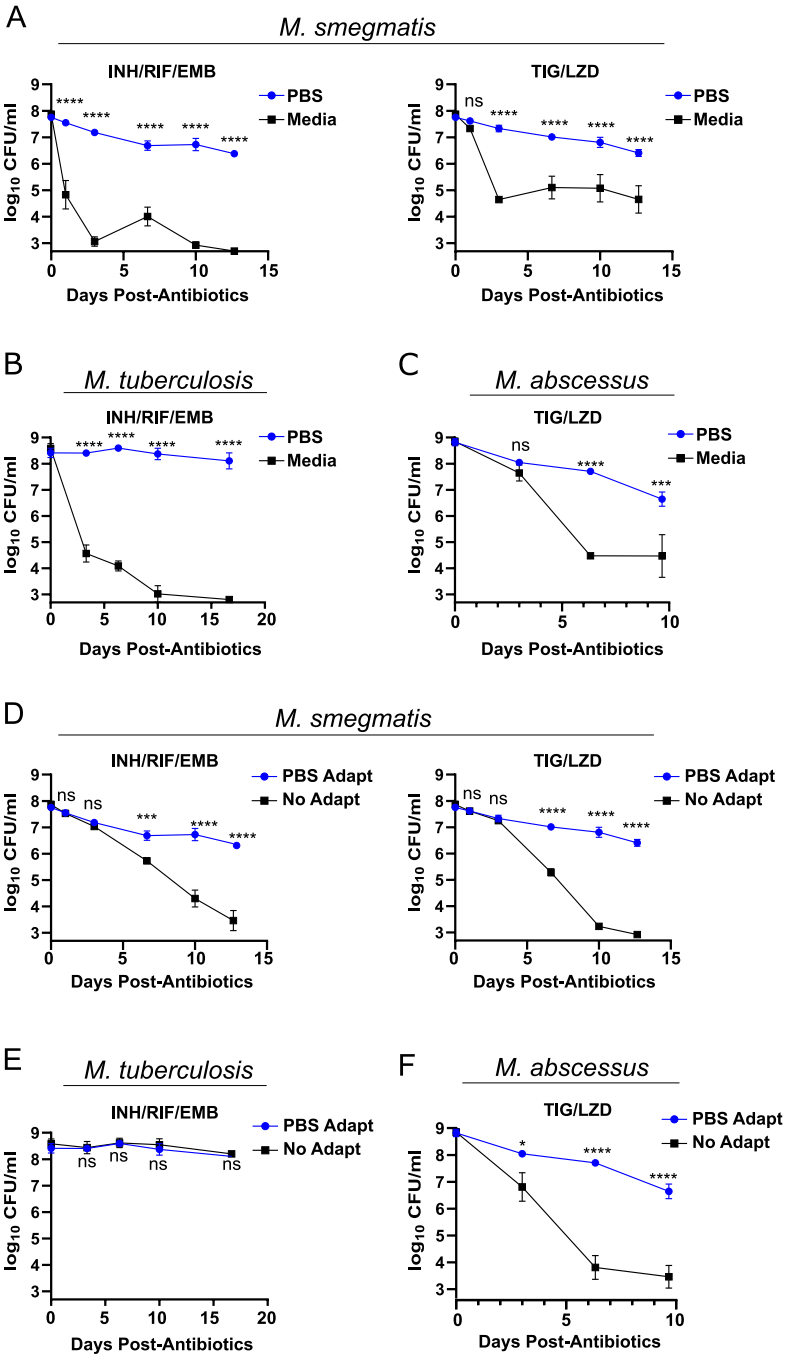
A
M. smegmatis
INH/RIF/EMB
TIG/LZD
PBS
Media
log10 CFU/ml
Days Post-Antibiotics
B
M. tuberculosis
C
M. abscessus
D
PBS Adapt
No Adapt
E
F

FIGURE 2

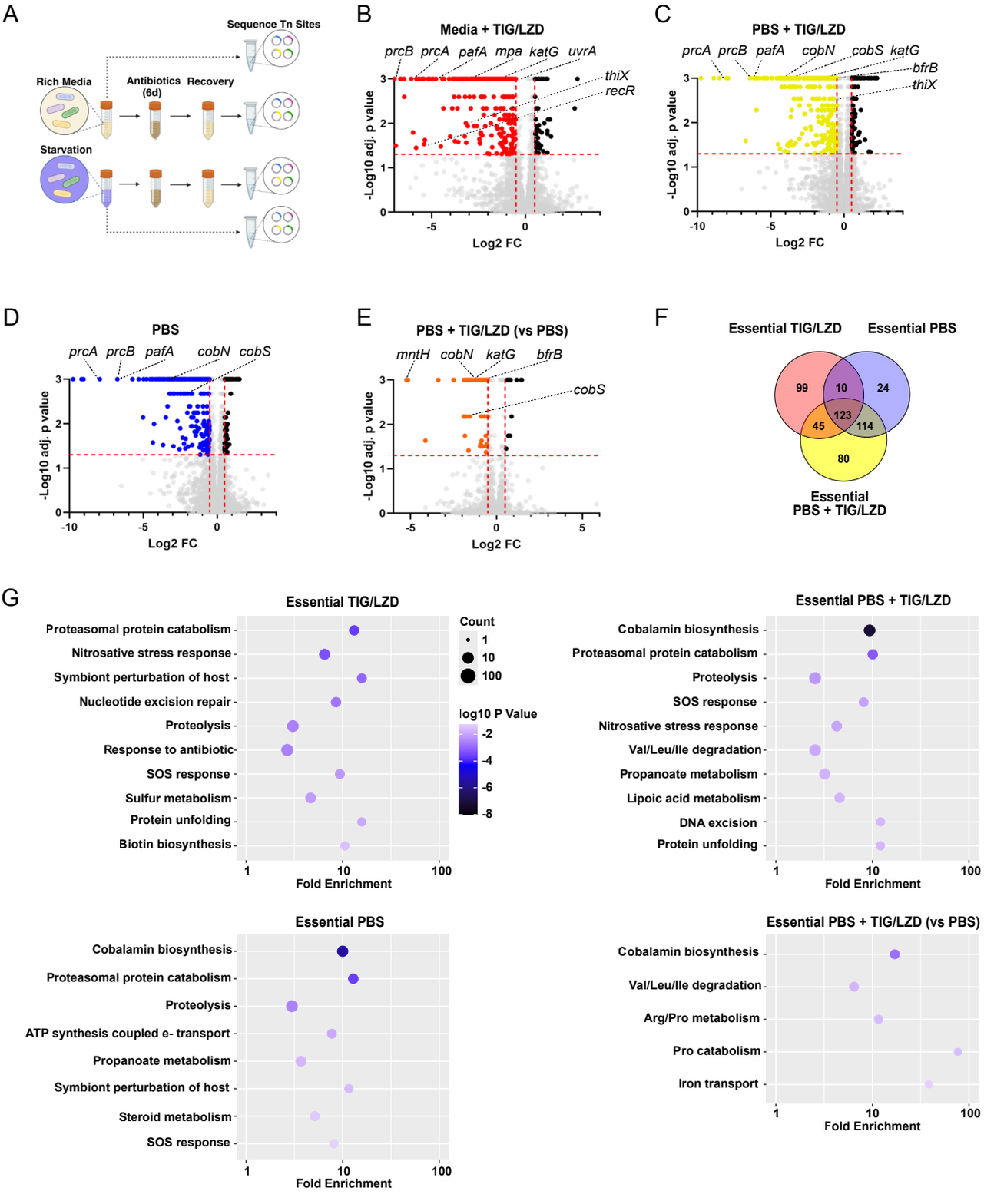
A
Sequence Tn Sites
Rich Media
Antibiotics (6d)
Recovery
Starvation
B
Media + TIG/LZD
prcB prcA pafA mpa katG uvrA
thiX
recR
-Log10 adj. p value
Log2 FC
C
PBS + TIG/LZD
prcA prcB pafA cobN cobS katG
bfrB
thiX
-Log10 adj. p value
Log2 FC
D
PBS
prcA prcB pafA cobN cobS
-Log10 adj. p value
Log2 FC
E
PBS + TIG/LZD (vs PBS)
mntH cobN katG bfrB
cobS
-Log10 adj. p value
Log2 FC
F
Essential TIG/LZD
Essential PBS
99
10
24
123
45
114
80
Essential PBS + TIG/LZD
G
Essential TIG/LZD
Proteasomal protein catabolism
Nitrosative stress response
Symbiont perturbation of host
Nucleotide excision repair
Proteolysis
Response to antibiotic
SOS response
Sulfur metabolism
Protein unfolding
Biotin biosynthesis
Fold Enrichment
Count
1
10
100
log10 P Value
-2
-4
-6
-8
Essential PBS + TIG/LZD
Cobalamin biosynthesis
Proteasomal protein catabolism
Proteolysis
SOS response
Nitrosative stress response
Val/Leu/Ile degradation
Propanoate metabolism
Lipoic acid metabolism
DNA excision
Protein unfolding
Fold Enrichment
Essential PBS
Cobalamin biosynthesis
Proteasomal protein catabolism
Proteolysis
ATP synthesis coupled e- transport
Propanoate metabolism
Symbiont perturbation of host
Steroid metabolism
SOS response
Fold Enrichment
Essential PBS + TIG/LZD (vs PBS)
Cobalamin biosynthesis
Val/Leu/Ile degradation
Arg/Pro metabolism
Pro catabolism
Iron transport
Fold Enrichment

FIGURE 3

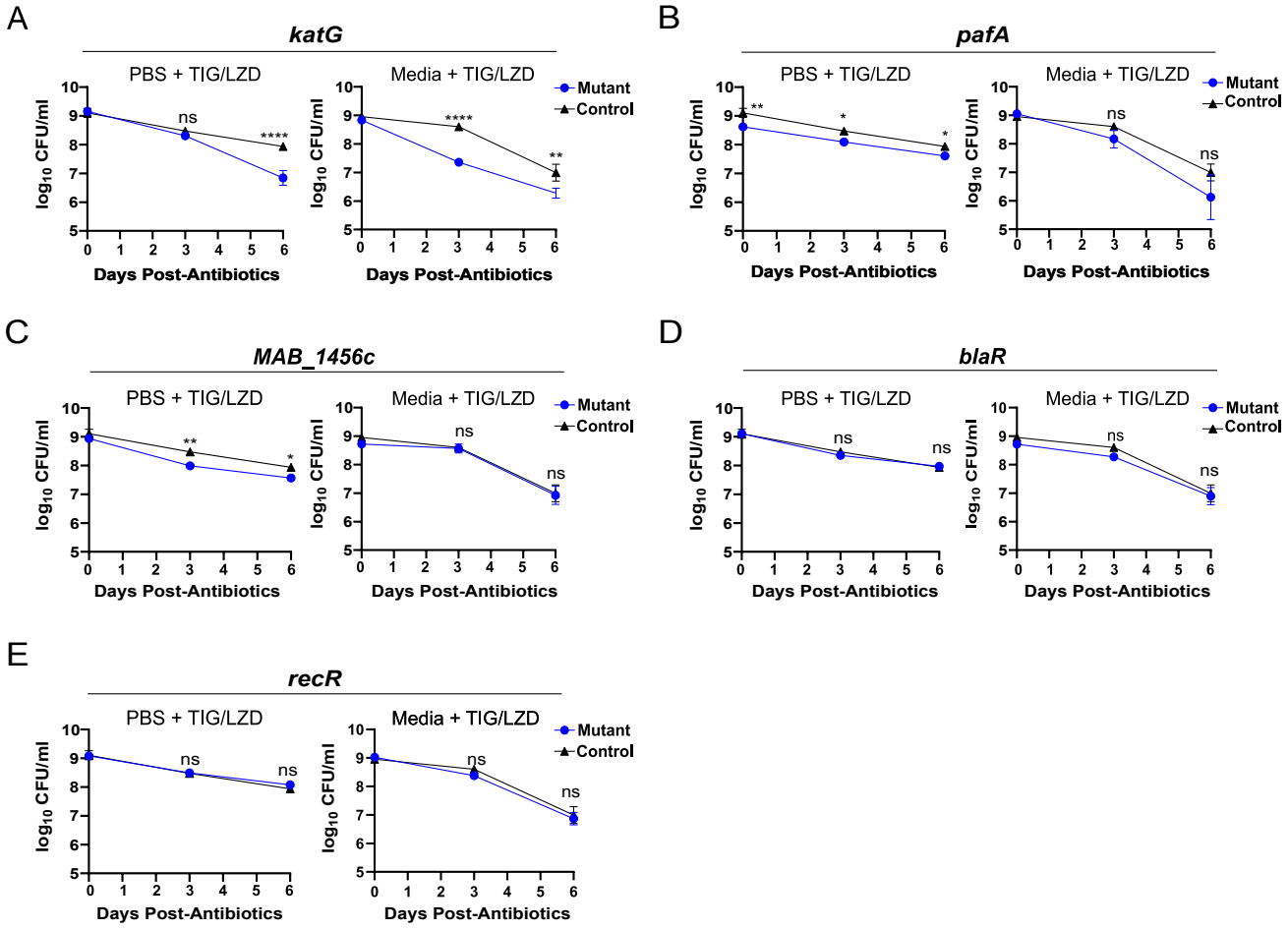
A
katG
PBS + TIG/LZD
Media + TIG/LZD
Mutant
Control
log10 CFU/ml
Days Post-Antibiotics
ns
****
**
B
pafA
PBS + TIG/LZD
Media + TIG/LZD
Mutant
Control
log10 CFU/ml
Days Post-Antibiotics
**
*
ns
C
MAB_1456c
PBS + TIG/LZD
Media + TIG/LZD
Mutant
Control
log10 CFU/ml
Days Post-Antibiotics
**
*
ns
D
blaR
PBS + TIG/LZD
Media + TIG/LZD
Mutant
Control
log10 CFU/ml
Days Post-Antibiotics
ns
E
recR
PBS + TIG/LZD
Media + TIG/LZD
Mutant
Control
log10 CFU/ml
Days Post-Antibiotics
ns

FIGURE 4

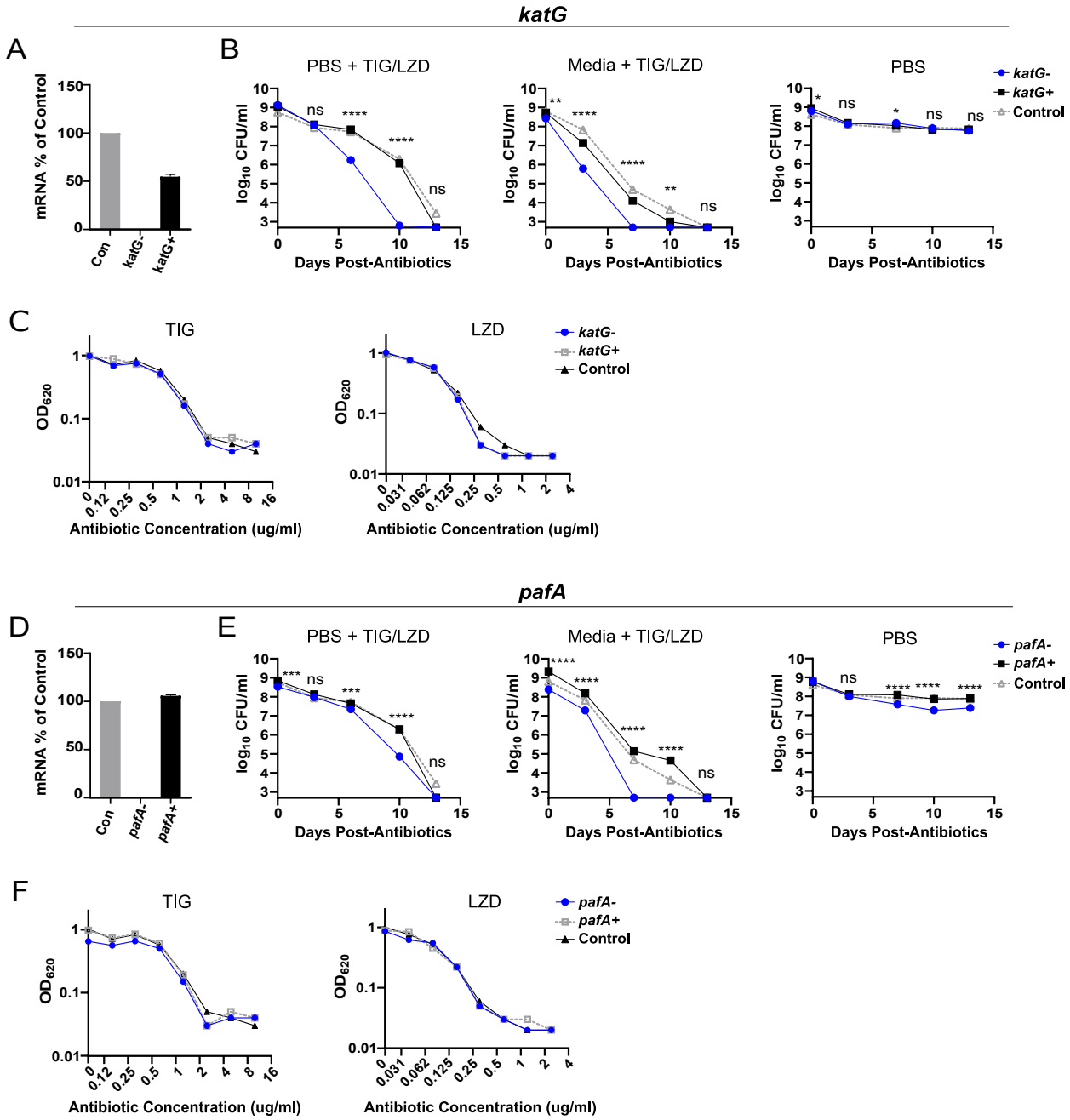
katG
A
mRNA % of Control
Con
katG-
katG+
B
PBS + TIG/LZD
Media + TIG/LZD
PBS
log10 CFU/ml
Days Post-Antibiotics
katG-
katG+
Control
C
TIG
LZD
OD620
Antibiotic Concentration (ug/ml)
pafA
D
E
pafA-
pafA+
F

FIGURE 5

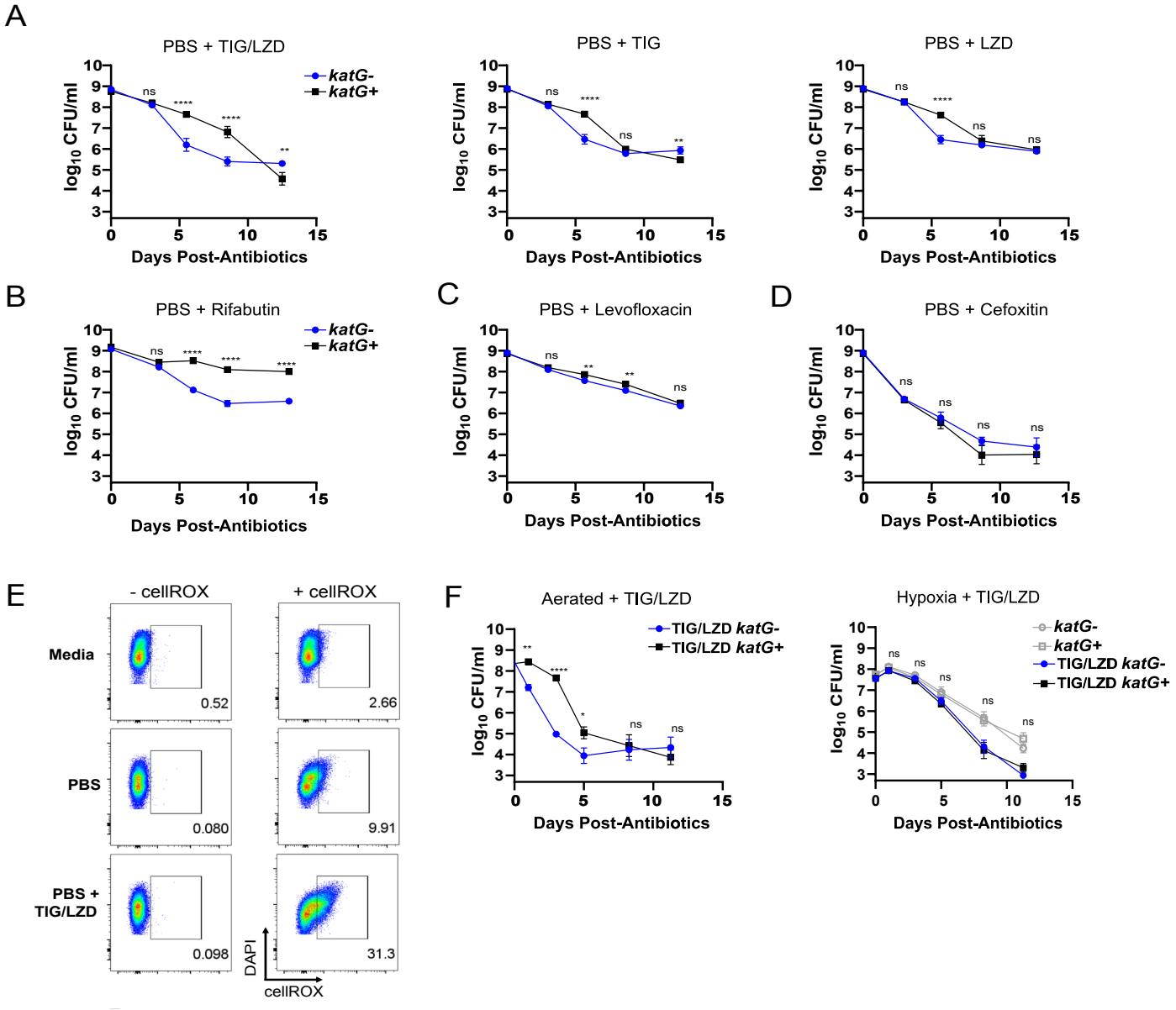
A
PBS + TIG/LZD
PBS + TIG
PBS + LZD
katG-
katG+
log10 CFU/ml
Days Post-Antibiotics
ns
****
**
B
PBS + Rifabutin
C
PBS + Levofloxacin
D
PBS + Cefoxitin
E
- cellROX
+ cellROX
Media
PBS
PBS + TIG/LZD
0.52
2.66
0.080
9.91
0.098
31.3
DAPI
cellROX
F
Aerated + TIG/LZD
Hypoxia + TIG/LZD
TIG/LZD katG-
TIG/LZD katG+
*

FIGURE 6

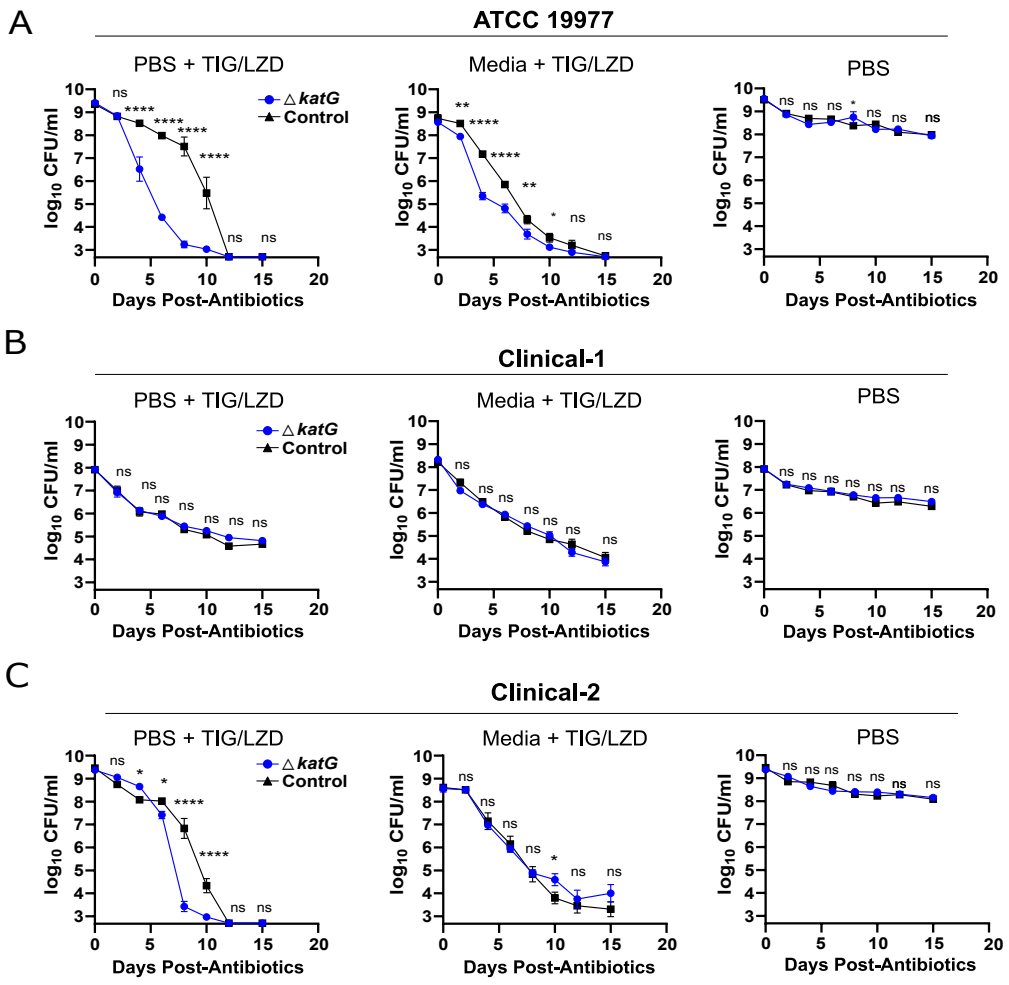
A
ATCC 19977
PBS + TIG/LZD
Media + TIG/LZD
PBS
△ katG
Control
log10 CFU/ml
Days Post-Antibiotics
B
Clinical-1
C
Clinical-2